HnRNPAB is an independent prognostic factor in non-small cell lung cancer and is involved in cell proliferation and metastasis

QINRONG WANG[1,2*], XUANJING GOU[1,2*], LINGLING LIU[1,2], TING ZHANG[1,2], HANG YUAN[3], YAN ZHAO[1,2], YUAN XIE[1,2], JIANJIANG ZHOU[1,2] and KEWEI SONG[1,2,4]

[1]Key Laboratory of Endemic and Ethnic Diseases, Guizhou Medical University, Ministry of Education; [2]Key Laboratory of Medical Molecular Biology, School of Basic Medicine, Guizhou Medical University, Guiyang, Guizhou 550004; [3]DNA Laboratory, Forensic Center of Public Security of Xiangyang, Xiangyang, Hubei 441000; [4]Department of Sport and Health, Guizhou Medical University, Guiyang, Guizhou 550004, P.R. China

Received November 18, 2022; Accepted March 15, 2023

DOI: 10.3892/ol.2023.13801

Abstract. Heterogeneous nuclear ribonucleoprotein A/B (hnRNPAB) is an RNA binding protein that is closely associated with the biological function and metabolism of RNA, which is involved in the malignant transformation of various tumor cells. However, the role and mechanisms of hnRNPAB in non-small cell lung cancer (NSCLC) are still unclear. In the present study, the expression levels of hnRNPAB in NSCLC and normal tissues were analyzed using the human protein atlas database and UALCAN database. The clinical significance of hnRNPAB was assayed using the data of NSCLC cases from The Cancer Genome Atlas database. Subsequently, two stable NSCLC cell lines with hnRNPAB knockdown were constructed and the effects of hnRNPAB silencing on cell viability, migration, invasion and epithelial-mesenchymal transition (EMT) were identified. Genes associated with hnRNPAB expression in NSCLC were screened using the Linked Omics database and verified by quantitative real-time PCR (RT-qPCR). The database analysis indicated that hnRNPAB was mainly expressed in the nucleus of NSCLC cells. Compared with the normal tissues, hnRNPAB expression was overexpressed in NSCLC tissues and was closely associated with the overall survival, sex, tumor-node-metastases classification, and poor prognosis of patients with lung adenocarcinoma. Functionally, knockdown of hnRNPAB inhibited the proliferation, migration, invasion and EMT of NSCLC cells and arrested the cell cycle at G_1 phase. Mechanistically, the bioinformatics analysis and RT-qPCR verification demonstrated that hnRNPAB knockdown led to a significant expression change of genes associated with tumorigenesis. In conclusion, the present study indicated that hnRNPAB played an important role in the malignant transformation of NSCLC, supporting the significance of hnRNPAB as a novel potential therapeutic target for the early diagnosis and prognosis of NSCLC.

Correspondence to: Professor Qinrong Wang or Professor Kewei Song, Key Laboratory of Endemic and Ethnic Diseases, Guizhou Medical University, Ministry of Education, 9 Beijing Road, Guiyang, Guizhou 550004, P.R. China
E-mail: qin_rong_fei@163.com
E-mail: 276979471@qq.com

*Contributed equally

Key words: non-small cell lung cancer, heterogeneous nuclear ribonucleoprotein A/B, RNA binding protein, cell proliferation, metastasis

Introduction

Lung cancer is one of the most common malignancies (1). For more than a decade, lung cancer has remained the leading cause of cancer death worldwide (1). Lung cancer is divided into small-cell lung cancer (SCLC) and non-small-cell lung cancer (NSCLC), of which NSCLC accounts for about 85-90% and mainly includes lung adenocarcinoma (LUAD) and lung squamous cell carcinoma (LUSC) (2). Although the overall treatment effect of patients has been improved with the continuous progress of diagnosis and treatment technology in recent years, the prognosis of lung cancer is still poor (2,3). Therefore, exploring the molecular mechanism of lung cancer pathogenesis and progression is necessary for improving the survival rate of patients with lung cancer.

Tumor invasion and metastasis are important reasons for the poor prognosis of patients with NSCLC (4). A critical intrinsic factor for epithelial tumors to infiltrate and metastasize is the epithelial-mesenchymal transition (EMT) of tumor cells, which can be abnormally activated at various stages of cancer progression and plays critical roles in cell growth, invasion, metastasis, and resistance to the therapy of NSCLC (5-7). Consequently, it is of great significance to find the key factors that activate EMT for the treatment of NSCLC.

Heterogeneous nuclear ribonucleoproteins (hnRNPs) are a kind of RNA binding proteins (RBPs) closely related to the function and metabolism of RNA, such as transcription, alternative splicing, nucleocytoplasmic transport, stability, and translation (8). Studies have shown that the dysregulation of hnRNPs expression is closely related to the EMT of

various malignant tumor cells (9). HnRNPAB is a member of the hnRNPs family. Zhou *et al* (10) and Yang *et al* (11) reported that hnRNPAB was overexpressed in hepatocellular carcinoma (HCC) and promoted the EMT of tumor cells by regulating the transcriptions of snail family transcriptional repressor 1 (SNAI1, SNAIL) and long-noncoding RNA (lncRNA) ELF209. In addition, the expression of hnRNPAB is increased in breast cancer, colon cancer, and gastric cancer, in which hnRNPAB could serve as a prognostic biomarker and therapeutic target (12-14). However, the function of hnRNPAB in NSCLC has not yet been reported.

In this study, the expression and localization of hnRNPAB in NSCLC tissues and its correlation with clinicopathological parameters of patients with NSCLC were analyzed through public databases. Then the role of hnRNPAB silencing in the malignant transformation of NSCLC cells was investigated *in vitro*, and finally the molecular mechanism of hnRNPAB promoting the proliferation and metastasis of NSCLC cells was investigated by bioinformatics and RT-qPCR. This study may contribute to discovering a new prognostic biomarker and therapeutic target for NSCLC patients.

Materials and methods

HnRNPAB expression analysis. The expression and localization of hnRNPAB in lung cancer and normal tissues were analyzed by the human protein atlas database (http://www.proteinatlas.org/) and UALCAN database (http://ualcan.path.uab.edu/). The data of 585 LUAD and 550 LUSC cases were downloaded from the TCGA database (https://tcga-data.nci.nih.gov/tcga/), including mRNA expression profile, sex, age, tumor-node-metastases (TNM) classification, and overall survival. The median expression level of hnRNPAB mRNA in 585 LUAD or 550 LUSC cases was used as the cutoff. Then the survival curve was drawn by the Kaplan-Meier method and compared by the log-rank test. The relationships between hnRNPAB expression and clinicopathological parameters were analyzed by the Chi-square (χ^2) test. Univariate and multivariate analyses of potential prognostic factors for overall survival were preformed using the Cox proportional hazard model. Genes associated with hnRNPAB expression in NSCLC were analyzed using the Linked Omics database (http://linkedomics.org/) based on the Pearson correlation coefficient.

Cell Culture. The human NSCLC cell line NCI-H292 and the human renal epithelial cell line 293T were purchased from Kunming Cell Bank of Chinese Academy of sciences. The human NSCLC cell line PC-9 was obtained from FuHeng Biology Company (Shanghai, China). NCI-H292 and PC-9 were maintained in RPMI-1640 medium (C11875500BT, Gibco, Thermo Fisher Scientific, Waltham, MA, USA) supplemented with 10% fetal bovine serum (10270-106, FBS, Gibco). 293T was cultured in Dulbecco's Modified Eagle Medium (DMEM, C11995500BT, Gibco) with 10% FBS. All cell lines were cultured at 37˚C in a 5% CO_2 humidified atmosphere.

Plasmid construction. To construct hnRNPAB knockdown recombinants, hnRNPAB and negative control (NC) shRNA sequences (sense and antisense) were designed (shown in Table I) and synthesized, which were dissolved in Tris-EDTA buffer to a final concentration of 100 μM. For each shRNA, the sense and antisense strands were mixed with a 1:1 ratio and then annealed through a PCR program (95˚C for 2 min, 72˚C for 2 min, 37˚C for 2 min, 25˚C for 2 min). The paired shRNA was cloned into the vector psi-LVRU6GP (GeneCopoeia, Germantown, MD, USA) digested with *Bam*H I and *Eco*R I (1010S and 1040S, Takara, Beijing, China). All constructs were confirmed by DNA sequencing (Sangon Biotech, Shanghai, China).

HnRNPAB knockdown. 293T cells were plated in a 6-well plate and the cell confluence reached 90% after 24 h. The hnRNPAB shRNA or NC shRNA recombinants, lentivirus packaging plasmid psPASX2 and PMD2G were mixed in a 4:3:1 ratio and then transfected into 293T cells using an Entranster™-R4000 reagent (4000-4, Engreen Biosystem, Beijing, China) following the manufacturer's instructions. At 48 h after transfection, the viral supernatant was collected and filtered with 0.22 μm filters. The virus solution was mixed with lentivirus infection reagent (30001-2-0.5, Engreen Biosystem) according to the manufacturer's instructions and then added into the NCI-H292 or PC-9 cells with a 40-60% cell confluence. After 8 h of lentivirus infection, the infection solution was replaced by fresh RPMI-1640 medium (10% FBS, no antibiotics). After 72 h of infection, puromycin (final concentration 2.0 μg/ml) was added to screen the stable cell lines.

Western blotting. Cells were lysed in RIPA buffer (P0013B, Beyotime, Shanghai, China) for 20 min on ice and then centrifuged at 12,000 x g for 10 min at 4˚C. The proteins in harvested supernatants were separated on 10% SDS-PAGE gels and then transferred onto polyvinylidene difluoride membranes (IPVH00010, Millipore, Merck, Billerica, MA, USA), which were successively probed with indicated antibodies and detected with an Enhanced Chemiluminescence Reagent (WBKLS0100, Millipore). Rabbit polyclonal antibodies against hnRNPAB (A17497, 1:2,000, ABclonal, Wuhan, China), Glyceraldehyde 3-phosphate dehydrogenase (GAPDH, 60004-1-Ig, 1:5,000, Proteintech, Wuhan, China), ZEB1 (21544-1-AP, 1:1,000, Proteintech), N-cadherin (22018-1-AP, 1:5,000, Proteintech), E-cadherin (20874-1-AP, 1:5,000, Proteintech), Vimentin (10366-1-AP, 1:10,000, Proteintech) and SNAI1 (13099-1-AP, 1:2,000, Proteintech), and a horseradish peroxidase-conjugated secondary antibody (SA00001-2, 1:5,000, Proteintech) were used.

Real-time quantitative PCR (RT-qPCR) analysis. Total RNA was extracted using a TRIzol reagent (15596-026, Invitrogen, Thermo Fisher Scientific) and reverse transcribed into cDNA by a PrimeScript™ RT reagent Kit with gDNA Eraser (RR047A, Takara). Fluorescence quantitative PCR was performed using a 2x SYBR Green quantitative PCR Master Mix (B21203, Bimake, Shanghai, China) according to the manufacturer's protocol in an Applied Biosystems StepOne Plus Real-Time PCR System (Applied Biosystems, Foster, CA, USA). The primer sequences of each gene were shown in Table I. GAPDH was used as a reference gene. The relative mRNA expression was calculated by the $2^{-\Delta\Delta Ct}$ method. All reactions were performed in triplicate.

Table I. Primer sequences.

Gene	Direction	Primer sequences (5'-3')
hnRNPAB (NM_004499) shRNA-1	Sense	GATCCGTGGAAGCAAGTGTGAGATCAATTCAA GAGATTGATCTCACACTTGCTTCCATTTTTTG
	Antisense	AATTCAAAAAATGGAAGCAAGTGTGAGATCAA TCTCTTGAATTGATCTCACACTTGCTTCCACG
hnRNPAB (NM_004499) shRNA-2	Sense	GATCCGGTTTGGGTTTATCCTGTTCATTCAAGA GATGAACAGGATAAACCCAAACCTTTTTTG
	Antisense	AATTCAAAAAAGGTTTGGGTTTATCCTGTTCA TCTCTTGAATGAACAGGATAAACCCAAACCG
NC shRNA	Sense	GATCCGCTTCGCGCCGTAGTCTTATTCAAG AGATAAGACTACGGCGCGAAGCTTTTTTG
	Antisense	AATTCAAAAAAGCTTCGCGCCGTAGTCTTA TCTCTTGAATAAGACTACGGCGCGAAGCG
hnRNPAB (NM_004499) qPCR	Sense	TTTGGCGAGTTTGGGGAGATT
	Antisense	GCCATACTGCTGCTGATAGAC
NOP16 (NM_001256539) qPCR	Sense	AAAGGAAATACTCTGTCTCGGG
	Antisense	CTTCTGCAAAGAATCGAGGAAG
DDX41 (NM_001321732) qPCR	Sense	CCACTACCTTCATCAACAAAGC
	Antisense	ACCTTCTGCTTGGCTTCTAG
NPM1 (NM_001355007) qPCR	Sense	AGTATATCTGGAAAGCGGTCTG
	Antisense	CATTTTTGGCTGGAGTATCTCG
TCOF1 (NM_001135243) qPCR	Sense	TTTGTCGACCCTAATCGTAGTC
	Antisense	CAGGAGTCAAGCACTGTGTAG
TMED9 (NM_017510) qPCR	Sense	GAGACCATGGTCATAGGAAACT
	Antisense	TATGGGAAGTGAAAGTGAACCT
CENPH (NM_022909) qPCR	Sense	TTCCAGAACCTTATTTTGGGGA
	Antisense	CTTCTCAAGCTGCAGAACAATT
CCNB1 (NM_001354844) qPCR	Sense	CTTGCAGTAAATGATGTGGATG
	Antisense	GTGACTTCCCGACCCAGTAG
PPM1G (NM_177983) qPCR	Sense	AACTCCTTCACAAGAAAATGGC
	Antisense	TGTCCTCAAAGAACTTGGACTT
SFXN1 (NM_001322977) qPCR	Sense	TGGGATCAAAGCACTTTCATTG
	Antisense	TTTCTGTAAGACCAGGAGGAAC
HSPA9 (NM_004134) qPCR	Sense	GTCAGATTGGAGCATTTGTGTT
	Antisense	CGAGTCATTGAAATAAGCTGGG
GAPDH (NM_001357943) qPCR	Sense	GGAGCGAGATCCCTCCAAAAT
	Antisense	GGCTGTTGTCATACTTCTCATGG
ZEB1 (NM_001128128) qPCR	Sense	TTACACCTTTGCATACAGAACCC
	Antisense	TTTACGATTACACCCAGACTGC
E-cadherin (NM_001317185) qPCR	Sense	CGAGAGCTACACGTTCACGG
	Antisense	GGGTGTCGAGGGAAAAATAGG
N-cadherin (NM_001308176) qPCR	Sense	AGCCAACCTTAACTGAGGAGT
	Antisense	GGCAAGTTGATTGGAGGGATG
Vimentin (NM_003380) qPCR	Sense	TGCCGTTGAAGCTGCTAACTA
	Antisense	CCAGAGGGAGTGAATCCAGATTA
SNAI1 (NM_005985) qPCR	Sense	ACTGCAACAAGGAATACCTCAG
	Antisense	GCACTGGTACTTCTTGACATCTG

CCK8 assay. Cells were seeded into 96-well plates at a concentration of $2x10^3$ cells per well and then cultured for 24, 48, and 72 h, respectively. At the indicated time, 10 μl CCK-8 solution was added to each well and mixed. The cells were incubated for 1-4 h at 37˚C and the absorbance at 450 nm was measured with a Biotek ELx800 (Biotek Winooski, Vermont, USA).

Adherent colony formation. Cells were seeded in 6-well plates at a concentration of $1x10^3$ cells per well and cultured for 2 weeks. The cells were washed twice with 1x phosphate buffered solution (PBS), fixed with 4% paraformaldehyde for 30 min, and stained with 0.01% crystal violet for 15 min. The number of colonies was counted using ImageJ.

Wound healing assay. Cells were plated in 6-well plates and reached confluence after 24 h. A straight wound was scratched on the cell layer with a 200 μl pipette. Then the cells were washed twice with 1x PBS and cultured in the medium with 4% FBS. The photographs were taken at 0 and 24 h for the same visual fields. Cell migration was expressed as the percentage of scratch healing, which was calculated by [(scratch area at 0 h-scratch area at 24 h)/scratch area at 0 h] x100%.

Invasion assay. The upper Transwell chamber (CLS3464, Corning Costar, Tewksbury, MA, USA) was coated with 100 μl 10% BD Matrigel matrix (356234, BD Biosciences, San Jose, CA, USA) diluted with the serum-free medium, and then incubated in a cell incubator for 2 h. $2x10^4$ cells per well suspended in the serum-free medium were plated into the upper chamber. The bottom chamber was filled with 700 μl medium containing 10% FBS. After incubation for 48 h, cells in the upper membrane of chamber were removed and cells adhering to the lower membrane were fixed with 4% paraformaldehyde for 30 min and stained with crystal violet for 15 min. Five random areas for each chamber were selected to count cell numbers.

Cell cycle analysis. Cells were collected, washed twice with precooled 1x PBS, and fixed overnight at 4˚C with 75% alcohol (diluted with 1x PBS). Then the cells were harvested again, washed twice with precooled PBS, and incubated with 500 μl staining solution (50 μg/ml propidium iodide, 100 μg/ml RNase A, 0.2% Triton X-100, 1x PBS) for 30 min. Cell-cycle was detected on a BD Accuri C6 flow cytometry (BD Biosciences, San Jose, CA, USA) and the results were analyzed with the software Modifit (Verity Software House, Topsham, ME, USA).

Cell apoptosis analysis. Cells were harvested and washed twice with precooled 1x PBS. After staining with Annexin V-APC and 7-AAD (AP105, MULTISCIENCES, Hangzhou, China), cells were analyzed on a BD Accuri C6 flow cytometry (BD Biosciences). All samples were assayed in triplicate.

Statistical analysis. Software SPSS 21.0 (IBM, Armonk, NY, USA) was used for the statistical analysis. Differences between two groups were determined by Student's t-test, and analysis of one-way ANOVA followed by the post hoc Dunnett's test was used for comparisons of more than two. Survival curves were analyzed by the Kaplan-Meier log-rank test. Genes expression correlation was analyzed using the Pearson correlation coefficient. Experiments were performed in triplicate. All experimental data are presented as the mean ± SD. P<0.05 indicates a statistically significant difference.

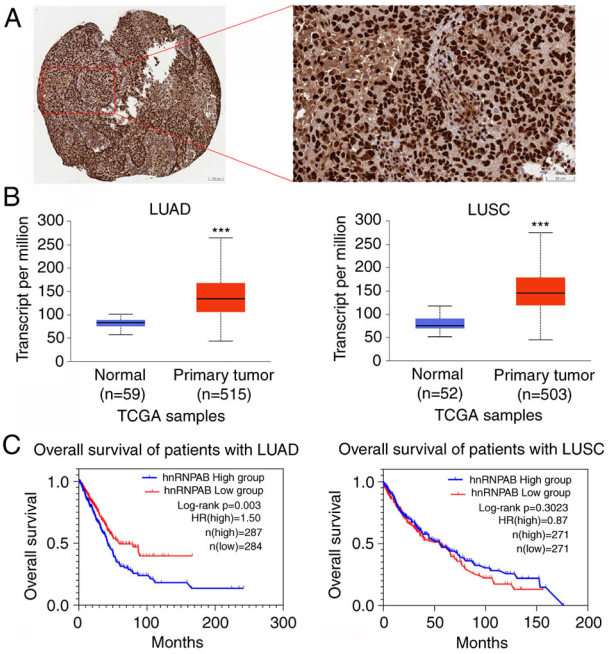

Figure 1. hnRNPAB expression is upregulated in NSCLC tissues and correlates with poor prognosis of patients with LUAD. (A) Localization of hnRNPAB protein in NSCLC tissues was analyzed using the human protein atlas database (left scale bar, 100 μm; right scale bar, 50 μm). (B) Expression levels of hnRNPAB in NSCLC and normal tissues were analyzed using the UALCAN database. (C) Prognostic effect of hnRNAPAB expression in NSCLC was analyzed using the Kaplan-Meier method and compared using the log-rank test. ***P<0.001 compared with normal group. hnRNPAB, heterogeneous nuclear ribonucleoprotein A/B; NSCLC, non-small cell lung cancer; LUAD, lung adenocarcinoma; LUSC, lung squamous cell carcinoma.

Results

HnRNPAB expression is up-regulated in NSCLC tissues and associated with the poor prognosis of patients. Firstly, the expression and role of hnRNPAB in NSCLC tissues were examined. Immunohistochemical staining (IHC) analysis from the human protein atlas database indicated that hnRNPAB protein was mainly expressed in the nucleus of NSCLC cells (Fig. 1A). Compared with normal tissues, hnRNPAB mRNA was highly expressed in both LUAD and LUSC tissues (Fig. 1B). Overall survival analysis showed that high hnRNPAB mRNA expression was significantly associated with a poor prognosis in the patients with LUAD (Fig. 1C). Moreover, hnRNPAB mRNA expression was strongly associated with the sex and TNM classification of patients with LUAD (Table II). Univariate and multivariate analyses indicated that hnNRPAB expression was an independent prognostic factor for patients with LUAD (Table III). Therefore, the analysis suggested that hnRNPAB may be a useful biomarker in the prognosis of patients with LUAD.

HnRNPAB silencing inhibits the proliferation of NSCLC cells. The role of hnRNPAB expression dysregulation in NSCLC cells was further explored by constructing two stable hnRNPAB knockdown cell lines. Compared with the control group (NC shRNA), hnRNPAB protein and mRNA expression levels in NCI-H292 and PC-9 cells with hnRNPAB knockdown (hnRNPAB shRNA-1 and shRNA-2) were

Table II. Correlations between hnRNPAB mRNA expression level and clinicopathological parameters in NSCLC.

	hnRNPAB expression in LUAD				hnRNPAB expression in LUSC			
Variable	Low (n=292)	High (n=293)	χ^2	P-value	Low (n=275)	High (n=275)	χ^2	P-value
Sex			6.419	0.011[a]			1.133	0.287
Female	119	150			208	197		
Male	173	143			67	78		
Age			1.410	0.235			1.029	0.310
≤60	94	108			58	68		
>60	198	185			217	207		
T classification			10.487	0.033[a]			4.077	0.253
T1	112	79			55	71		
T2	150	171			172	151		
T3	21	29			38	39		
T4	7	13			10	14		
T_X	2	1			0	0		
N classification			13.298	0.010[a]			2.258	0.688
N0	194	178			181	170		
N1	46	61			65	79		
N2	38	49			23	20		
N3	0	2			2	3		
N_X	14	3			4	3		
M classification			6.050	0.049[a]			3.144	0.208
M0	188	212			227	221		
M1	12	15			6	2		
M_X	92	66			42	52		

[a]P<0.05 analyzed by χ^2 test. hnRNPAB, heterogeneous nuclear ribonucleoprotein A/B; LUAD, lung adenocarcinoma; LUSC, lung squamous cell carcinoma.

significantly reduced (Fig. 2A). CCK-8 and adherent colony formation assays indicated that hnRNPAB knockdown decreased cell viability and proliferation (Fig. 2B and C). In addition, the flow cytometry showed that silencing of hnRNPAB arrested the cell cycle at G_0/G_1 phase but did not promote cell apoptosis, which indicated that hnRNPAB silence suppressed cell proliferation by arresting the cell cycle at G_0/G_1 phase (Figs. 2D and S1).

HnRNPAB knockdown inhibits cell migration, invasion, and EMT of NSCLC. Next, the effects of hnRNPAB knockdown on cell migration, invasion, and EMT were detected. The scratch test showed that the wound healing degree of hnRNPAB shRNA group was significantly lower than that of NC shRNA group (Fig. 3A). The invasion assay showed that the cell number passing through the Matrigel matrix in hnRNPAB shRNA group was obviously less than that in NC shRNA group (Fig. 3B). Western blotting and RT-qPCR showed that the protein and mRNA expression levels of EMT-related markers ZEB1, SNAI1, N-cadherin and Vimentin in hnRNPAB shRNA group were decreased, while the protein and mRNA expression levels of E-cadherin were increased (Fig. 3C). Collectively, the results suggested that hnRNPAB knockdown significantly inhibited the migration, invasion, and EMT of NSCLC cells.

Analysis of genes related to hnRNPAB expression in NSCLC. To explore the molecular mechanism of hnRNPAB promoting the malignant transformation of NSCLC cells, the genes related to hnRNPAB expression in NSCLC were analyzed using the LinkedOmics database. As shown in Fig. 4A and B, the expressions of 9764 genes were positively correlated with the expression of hnRNPAB, and 10214 genes were negatively correlated with hnRNPAB. Several hnRNPAB-positive correlated genes with high Pearson Correlations that have been reported to be associated with tumorigenesis were screened to perform the co-expression analysis with hnRNPAB using the mRNA expression data of 585 LUAD and 550 LUSC samples obtained from the TCGA database, including NOP16 nucleolar protein (NOP16), nucleophosmin 1 (NPM1), treacle ribosome biogenesis factor 1 (TCOF1), centromere protein H (CENPH), cyclin B1 (CCNB1), heat shock protein family A (Hsp70) member 9 (HSPA9), sideroflexin 1 (SFXN1), protein phosphatase, Mg^{2+}/Mn^{2+} dependent 1G (PPM1G), transmembrane p24 trafficking protein 9 (TMED9), and DEAD-box helicase 41 (DDX41) (15-26). As shown in Fig. 4C, the screened 10 genes

Table III. Univariate and multivariate analyses of various prognostic parameters in patients with LUAD.

Variable	Number of patients	Univariate analysis			Multivariate analysis		
		HR	95% CI	P-value	HR	95% CI	P-value
Sex		0.905	0.690-1.186	0.468	0.935	0.706-1.239	0.640
Female	262						
Male	309						
Age		1.236	0.925-1.653	0.151	1.191	0.889-1.1594	0.242
≤60	192						
>60	379						
T classification		1.511	1.285-1.776	0.000[a]	1.340	1.136-1.581	0.001[b]
T1	189						
T2	312						
T3	48						
T4	19						
T_X	3						
N classification		1.338	1.192-1.503	0.000[a]	1.298	1.142-1.474	0.000[a]
N0	365						
N1	106						
N2	82						
N3	2						
N_X	16						
M classification		0.943	0.803-1.107	0.471	1.0121	0.857-1.194	0.890
M0	387						
M1	26						
M_X	158						
hnRNPAB		1.509	1.147-1.984	0.003[b]	1.505	1.138-1.989	0.004[b]
Low	287						
High	284						

[a]P<0.001 and [b]P<0.01 by Cox proportional hazard model. HR, hazard ratio; CI, confidence interval; hnRNPAB, heterogeneous nuclear ribonucleoprotein A/B; LUAD, lung adenocarcinoma.

were positively co-expressed with hnRNPAB in both LUAD and LUSC samples. Moreover, the expressions of these genes were verified in hnRNPAB knockdown cells using RT-qPCR technology and the results showed that 5 genes except for HSPA9, SFXN1, PPM1G, TMED9, and DDX41 were down-regulated (Figs. 5 and S2), suggesting that hnRNPAB may promote the proliferation, migration, invasion, and EMT of NSCLC cells partially by up-regulating the expressions of these 5 genes.

Discussion

NSCLC has seriously threatened human health. Once NSCLC was diagnosed, most patients usually were in the late stage or their tumors have metastasized, thus losing the opportunity for surgery (27). Therefore, finding new diagnostic and therapeutic targets is of great importance to improve the survival rate of NSCLC patients.

HnRNPs are a kind of RNA binding proteins. So far, more than 20 hnRNP members have been identified, including hnRNPA ~ U (28). With the deepening of the research, it is found that hnRNP members have been involved in the development and progression of tumors by regulating cell proliferation, metastasis, self-renewal of cancer stem cells and so on (9). For example, hnRNPL promotes the progression of prostate cancer by regulating circCSPP1/microRNA-520h/early growth response factor 1 (EGR1) axis (29). HnRNPA1, A2/B1, and K binding to the promoter of the tumor suppressor Annexin A7 (ANXA7) alter the splicing pattern of ANXA7, leading to the progression of prostate cancer (30).

HnRNPAB is a member of the hnRNP family. Previous studies have shown that hnRNPAB is dysregulated in multiple tumors, which is associated with various malignant phenotypes of tumors (10-12,31). However, the expression and role of hnRNPAB in NSCLC remain unclear. According to our results, hnRNPAB exhibited a relatively high expression in NSCLC samples, showing significant correlation with the overall survival, sex and TNM classification of patients with LUAD. Multivariate Cox regression analysis pointed toward hnRNPAB as an independent prognostic marker. These

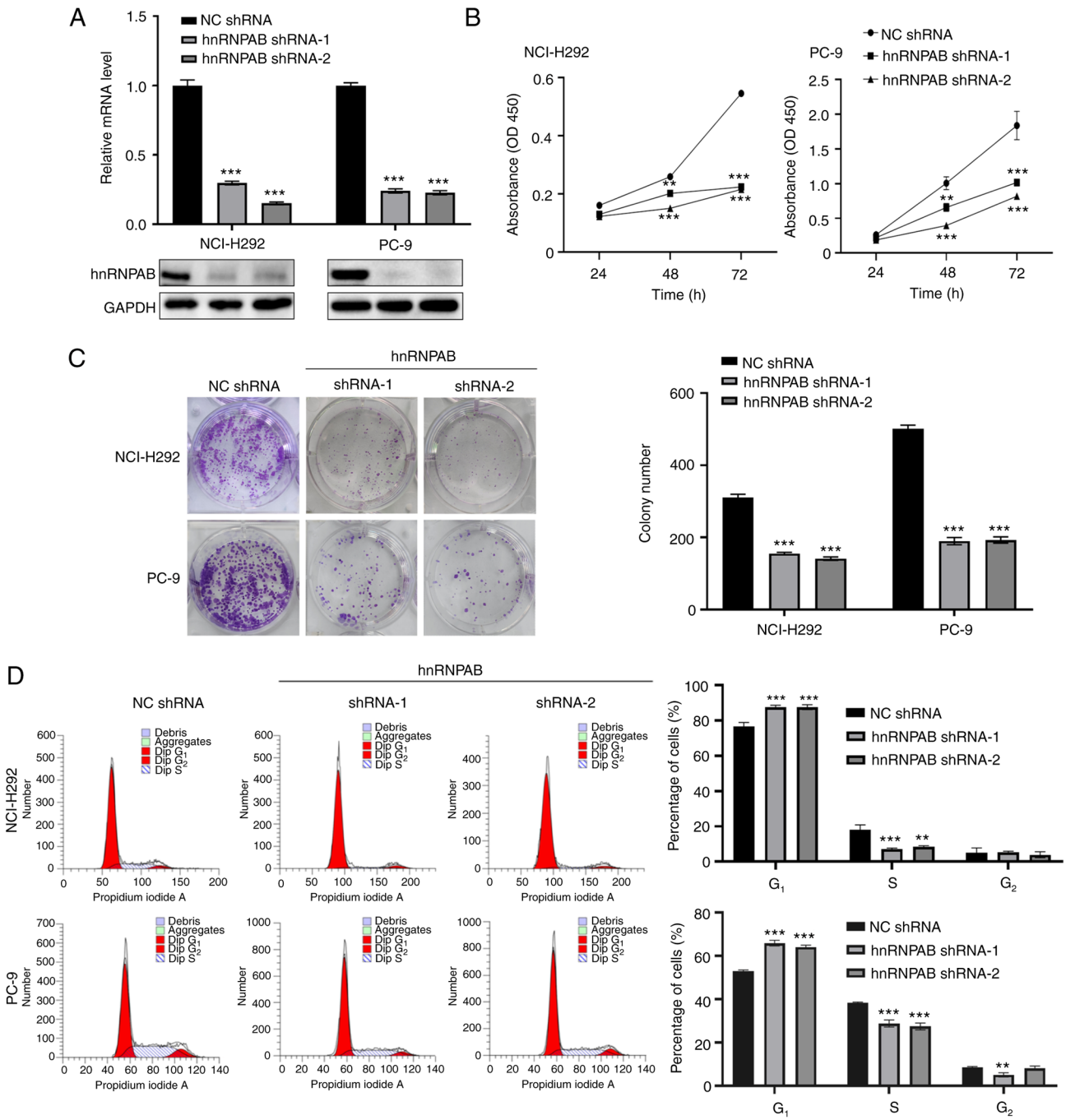

Figure 2. HnRNPAB knockdown inhibits the proliferation of non-small cell lung cancer cells. (A) Protein and mRNA expression levels of hnRNPAB in stable hnRNPAB knockdown cells were examined using western blotting and reverse transcription-quantitative PCR. GAPDH was used as an internal control. (B) Cell viability and (C) proliferation were tested by Cell Counting Kit-8 and adherent colony formation assays. (D) Cell cycle was detected using flow cytometry. Results are representative of three independent experiments. **P<0.01 and ***P<0.001 compared with NC shRNA. HnRNPAB, heterogeneous nuclear ribonucleoprotein A/B; NC, negative control; shRNA, short hairpin RNA; OD, optical density.

results suggested that hnRNPAB may play an important role in NSCLC progression.

Metastasis is a main cause of mortality in cancer patients (32). EMT is often activated during tumor metastasis (32). EMT is a reversible biological cellular process in which cells transform from an epithelial form to a mesenchymal form (7). In the process of EMT, the expressions of many mesenchymal related proteins are often increased, especially Vimentin (33). Cells in EMT acquire stem cell-like properties, in which the protein expression changed from E-cadherin to N-cadherin, ZEB1 and SNAI1, of which ZEB1 and SNAI1 directly suppressed the expression of E-cadherin by binding to its promoter (34-36). Our results showed that hnRNPAB knockdown increased the expression of E-cadherin and reduced the expressions of ZEB1, N-cadherin, Vimentin, and SNAI1, indicating EMT was reversed. In general, cancer cells obtain stronger proliferation, migration, and invasion abilities after EMT (37,38). Consistently, hnRNPAB silencing inhibited the proliferation, migration, and invasion of NSCLC cells. These observations suggested that hnRNPAB contributes

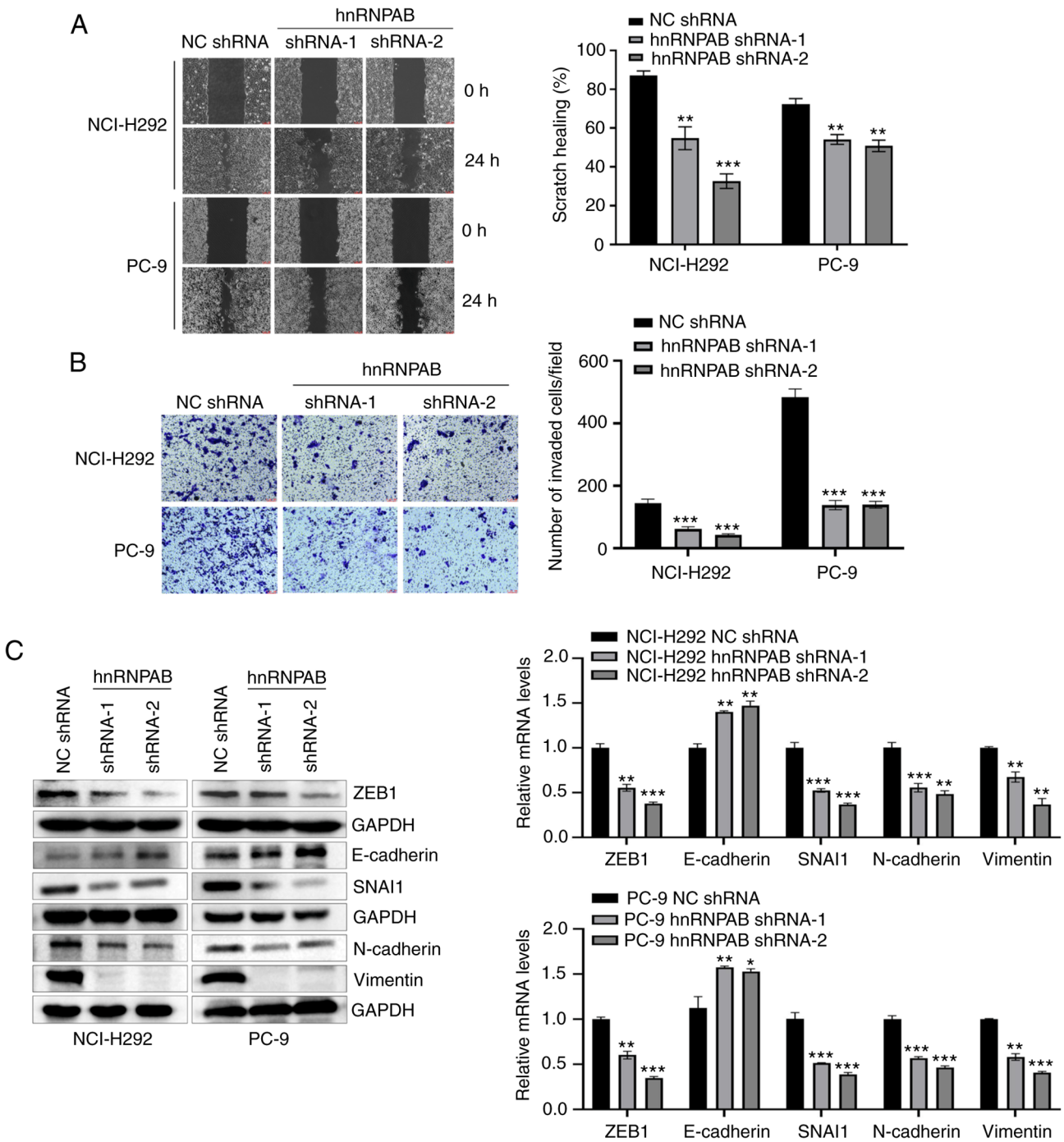

Figure 3. HnRNPAB-silencing inhibits the migration, invasion and EMT of NSCLC cells. (A) Cell migration was evaluated using wound healing assay (magnification, x100). (B) Cell invasion was evaluated using Matrigel matrix-coated Transwell assay (magnification, x100). (C) Protein and mRNA expression levels of EMT-related markers ZEB1, E-cadherin, SNAI1, N-cadherin and Vimentin were determined using western blotting and reverse transcription-quantitative-PCR. GAPDH was used as a loading control. For western blotting, multiple membranes from the same sample at the same time were used to expose different target proteins and so >1 GAPDH were provided. Results are representative of three independent experiments. *P<0.05, **P<0.01 and ***P<0.001 compared with respective NC shRNA group. HnRNPAB, heterogeneous nuclear ribonucleoprotein A/B; NC, negative control; shRNA, short hairpin RNA; EMT, epithelial-mesenchymal transition; ZEB1, zinc finger E-box binding homeobox 1.

to tumor progression, probably via the process of tumor proliferation and metastasis.

To explore the molecular mechanism of hnRNPAB regulating the proliferation and metastasis of NSCLC cells, 10 genes positively correlated with hnRNPAB expression were selected for verification. The results showed that the expressions of NOP16, NPM1, TCOF1, CENPH and CCNB1 were not only positively correlated with the expression of hnNRPAB in LUAD and LUSC cases but also down-regulated in hnRNPAB silenced cells. Previous studies have shown that these 5 genes were highly expressed in a variety of tumor tissues, which promoted the malignant transformation of tumor cells (15-18,21). Increased rRNA production is a hallmark of cancer (15,39). It is verified that NOP16 and TCOF1 could coordinate the production of rRNA to promote HCC and breast cancer tumorigenesis (15,39). NPM1 is a well-known

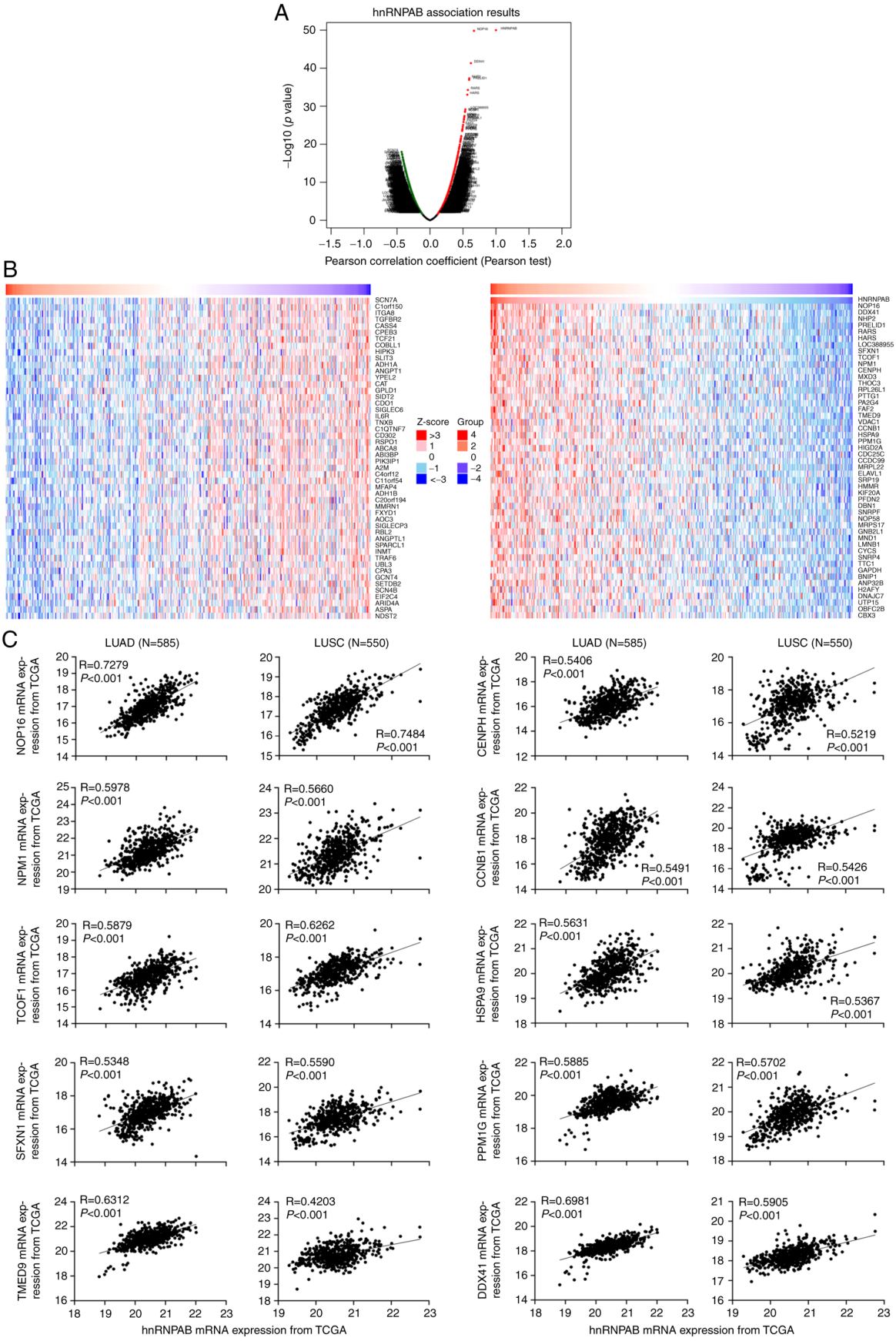

Figure 4. Analysis of genes related to hnRNPAB expression in NSCLC. (A) Analysis of hnRNPAB-related genes using LinkedOmics database based on Pearson correlation coefficient. (B) Analysis of positive and negative correlated genes with hnRNPAB. (C) Co-expression analysis between hnRNPAB and the screened genes using the mRNA expression data of NSCLC samples from The Cancer Genome Atlas database. HnRNPAB, heterogeneous nuclear ribonucleoprotein A/B; NSCLC, non-small cell lung cancer; LUAD, lung adenocarcinoma; LUSC, lung squamous cell carcinoma; NOP16, NOP16 nucleolar protein; NPM1, nucleophosmin 1; TCOF1, treacle ribosome biogenesis factor 1; CENPH, centromere protein H; CCNB1, cyclin B1; HSP, heat shock protein family; SFXN1, sideroflexin 1; PPM1G, protein phosphatase, Mg^{2+}/Mn^{2+} dependent 1G; TMED9, transmembrane p24 trafficking protein 9; DDX41, DEAD-box helicase 41.

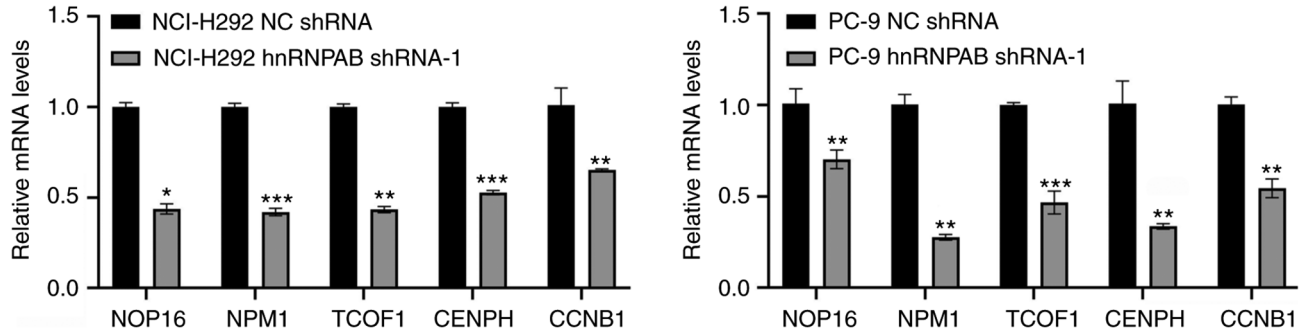

Figure 5. Expression levels of the screened genes in stable hnRNPAB-silenced cells were verified using RT-qPCR. The total RNA was extracted and the mRNA expression levels of NOP16, NPM1, TCOF1, CENPH and CCNB1 in stable non-small cell lung cancer cell lines were determined using RT-qPCR. GAPDH was used as an internal control. Results are representative of three independent experiments. *P<0.05, **P<0.01 and ***P<0.001 compared with respective NC shRNA group. HnRNPAB, heterogeneous nuclear ribonucleoprotein A/B; RT-qPCR, reverse transcription-quantitative PCR; NOP16, NOP16 nucleolar protein; NPM1, nucleophosmin 1; TCOF1, treacle ribosome biogenesis factor 1; CENPH, centromere protein H; CCNB1, cyclin B1; NC, negative control; shRNA, short hairpin RNA.

nucleocytoplasmic shuttling protein and its overexpression, translocation, mutation, or loss of function can lead to cancer and tumorigenesis (16). CENPH is highly expressed in NSCLC and may be used as a prognostic biomarker for patients with NSCLC (40). Likewise, CCNB1 is overexpressed in LUAD and involved in the proliferation and metastasis of tumor cells (21). These analyses indicate that hnRNPAB may promote the cell proliferation and metastasis of NSCLC by up-regulating the expressions of NOP16, NPM1, TCOF1, CENPH and CCNB1.

In conclusion, this study identified hnRNPAB as a useful biomarker in the prognosis of patients with LUAD. The overexpression of hnRNPAB promoted the proliferation and metastasis of NSCLC cells partially by up-regulating the expressions of NOP16, NPM1, TCOF1, CENPH and CCNB1. Our results may offer a potential novel target for the treatment of NSCLC.

Acknowledgements

Not applicable.

Funding

This work was supported by the National Natural Science Foundation of China (grant no. 81660474), the Guizhou Provincial Science and Technology Project [grant no. ZK(2022)041], the Academic Seedling Project of Guizhou Medical University (grant no. 19NSP009) and the Natural Science Foundation of Guizhou Provincial Health Commission (grant no. gzwkj2023-254).

Availability of data and materials

The datasets used and/or analyzed during the current study are available from the corresponding author on reasonable request.

Authors' contributions

QW and KS designed the research and confirmed the authenticity of all the raw data. XG performed experiments. XG, LL and HY performed statistical analysis. QW wrote the manuscript. QW and XG prepared figures. TZ, YZ, YX and JZ interpreted the data. All authors read and approved the final manuscript.

Ethics approval and consent to participate

Not applicable.

Patient consent for publication

Not applicable.

Competing interests

The authors declare that they have no competing interests.

References

1. Oliver AL: Lung cancer: Epidemiology and screening. Surg Clin North Am 102: 335-344, 2022.
2. Passiglia F, Bertaglia V, Reale ML, Delcuratolo MD, Tabbò F, Olmetto E, Capelletto E, Bironzo P and Novello S: Major breakthroughs in lung cancer adjuvant treatment: Looking beyond the horizon. Cancer Treat Rev 101: 102308, 2021.
3. Passiglia F, Pilotto S, Facchinetti F, Bertolaccini L, Del Re M, Ferrara R, Franchina T, Malapelle U, Menis J, Passaro A, *et al*: Treatment of advanced non-small-cell lung cancer: The 2019 AIOM (Italian Association of Medical Oncology) clinical practice guidelines. Crit Rev Oncol Hematol 146: 102858, 2020.
4. Bakir B, Chiarella AM, Pitarresi JR and Rustgi AK: EMT, MET, plasticity, and tumor metastasis. Trends Cell Biol 30: 764-776, 2020.
5. O'Leary K, Shia A and Schmid P: Epigenetic regulation of EMT in non-small cell lung cancer. Curr Cancer Drug Targets 18: 89-96, 2018.
6. Yuan X, Wu H, Han N, Xu H, Chu Q, Yu S, Chen Y and Wu K: Notch signaling and EMT in non-small cell lung cancer: Biological significance and therapeutic application. J Hematol Oncol 7: 87, 2014.
7. Mittal V: Epithelial mesenchymal transition in tumor metastasis. Annu Rev Pathol 13: 395-412, 2018.
8. Geuens T, Bouhy D and Timmerman V: The hnRNP family: Insights into their role in health and disease. Hum Genet 135: 851-867, 2016.
9. Han N, Li W and Zhang M: The function of the RNA-binding protein hnRNP in cancer metastasis. J Cancer Res Ther 9 (Suppl): S129-S134, 2013.

10. Zhou ZJ, Dai Z, Zhou SL, Hu ZQ, Chen Q, Zhao YM, Shi YH, Gao Q, Wu WZ, Qiu SJ, *et al*: HNRNPAB induces epithelial-mesenchymal transition and promotes metastasis of hepatocellular carcinoma by transcriptionally activating SNAIL. Cancer Res 74: 2750-2762, 2014.
11. Yang Y, Chen Q, Piao HY, Wang B, Zhu GQ, Chen EB, Xiao K, Zhou ZJ, Shi GM, Shi YH, *et al*: HNRNPAB-regulated lncRNA-ELF209 inhibits the malignancy of hepatocellular carcinoma. Int J Cancer 146: 169-180, 2020.
12. Cao Y, Zhang W, Jin YT and Zou Q: Mining the prognostic value of HNRNPAB and its function in breast carcinoma. Int J Genomics 2020: 3750673, 2020.
13. Pan T, Yu Z, Jin Z, Wu X, Wu A, Hou J, Chang X, Fan Z, Li J, Yu B, *et al*: Tumor suppressor lnc-CTSLP4 inhibits EMT and metastasis of gastric cancer by attenuating HNRNPAB-dependent Snail transcription. Mol Ther Nucleic Acids 23: 1288-1303, 2021.
14. Chen ZQ, Yuan T, Jiang H, Yang YY, Wang L, Fu RM, Luo SQ, Zhang T, Wu ZY and Wen KM: MicroRNA-8063 targets heterogeneous nuclear ribonucleoprotein AB to inhibit the self-renewal of colorectal cancer stem cells via the Wnt/β-catenin pathway. Oncol Rep 46: 219, 2021.
15. Zhang C, Yin C, Wang L, Zhang S, Qian Y, Ma J, Zhang Z, Xu Y and Liu S: HSPC111 governs breast cancer growth by regulating ribosomal biogenesis. Mol Cancer Res 12: 583-594, 2014.
16. Karimi Dermani F, Gholamzadeh Khoei S, Afshar S and Amini R: The potential role of nucleophosmin (NPM1) in the development of cancer. J Cell Physiol 236: 7832-7852, 2021.
17. Hu J, Lai Y, Huang H, Ramakrishnan S, Pan Y, Ma VWS, Cheuk W, So GYK, He Q, Geoffrey Lau C, *et al*: TCOF1 upregulation in triple-negative breast cancer promotes stemness and tumour growth and correlates with poor prognosis. Br J Cancer 126: 57-71, 2022.
18. Lu G, Shan T, He S, Ren M, Zhu M, Hu Y, Lu X and Zhang D: Overexpression of CENP-H as a novel prognostic biomarker for human hepatocellular carcinoma progression and patient survival. Oncol Rep 30: 2238-2244, 2013.
19. He WL, Li YH, Yang DJ, Song W, Chen XL, Liu FK, Wang Z, Li W, Chen W, Chen CY, *et al*: Combined evaluation of centromere protein H and Ki-67 as prognostic biomarker for patients with gastric carcinoma. Eur J Surg Oncol 39: 141-149, 2013.
20. Wu X, Lin Y, Shi L, Huang Y, Lai C, Wang Y, Zhang M, Wang S, Heng B, Yu G, *et al*: Upregulation of centromere protein H is associated with progression of renal cell carcinoma. J Mol Histol 46: 377-385, 2015.
21. Bao B, Yu X and Zheng W: MiR-139-5p targeting CCNB1 modulates proliferation, migration, invasion and cell cycle in lung adenocarcinoma. Mol Biotechnol 64: 852-860, 2022.
22. Guan Y, Zhu X, Liang J, Wei M, Huang S and Pan X: Upregulation of HSPA1A/HSPA1B/HSPA7 and downregulation of HSPA9 were related to poor survival in colon cancer. Front Oncol 11: 749673, 2021.
23. Chen L, Kang Y, Jiang Y, You J, Huang C, Xu X and Chen F: Overexpression of SFXN1 indicates poor prognosis and promotes tumor progression in lung adenocarcinoma. Pathol Res Pract 237: 154031, 2022.
24. Chen D, Zhao Z, Chen L, Li Q, Zou J and Liu S: PPM1G promotes the progression of hepatocellular carcinoma via phosphorylation regulation of alternative splicing protein SRSF3. Cell Death Dis 12: 722, 2021.
25. Han GH, Yun H, Chung JY, Kim JH and Cho H: TMED9 expression level as a biomarker of epithelial ovarian cancer progression and prognosis. Cancer Genomics Proteomics 19: 692-702, 2022.
26. Weinreb JT and Bowman TV: Clinical and mechanistic insights into the roles of DDX41 in haematological malignancies. FEBS Lett 596: 2736-2745, 2022.
27. Wenk MR and Choi H: Abundant circulating lipids-a new opportunity for NSCLC detection? Nat Rev Clin Oncol 19: 361-362, 2022.
28. Xie W, Zhu H, Zhao M, Wang L, Li S, Zhao C, Zhou Y, Zhu B, Jiang X, Liu W and Ren C: Crucial roles of different RNA-binding hnRNP proteins in Stem Cells. Int J Biol Sci 17: 807-817, 2021.
29. Lu J, Zhong C, Luo J, Shu F, Lv D, Liu Z, Tan X, Wang S, Wu K, Yang T, *et al*: HnRNP-L-regulated circCSPP1/miR-520h/EGR1 axis modulates autophagy and promotes progression in prostate cancer. Mol Ther Nucleic Acids 26: 927-944, 2021.
30. Torosyan Y, Dobi A, Glasman M, Mezhevaya K, Naga S, Huang W, Paweletz C, Leighton X, Pollard HB and Srivastava M: Role of multi-hnRNP nuclear complex in regulation of tumor suppressor ANXA7 in prostate cancer cells. Oncogene 29: 2457-2466, 2010.
31. Lu Y, Wang X, Gu Q, Wang J, Sui Y, Wu J and Feng J: Heterogeneous nuclear ribonucleoprotein A/B: An emerging group of cancer biomarkers and therapeutic targets. Cell Death Discov 8: 337, 2022.
32. Fares J, Fares MY, Khachfe HH, Salhab HA and Fares Y: Molecular principles of metastasis: A hallmark of cancer revisited. Signal Transduct Target Ther 5: 28, 2020.
33. Ostrowska-Podhorodecka Z and McCulloch CA: Vimentin regulates the assembly and function of matrix adhesions. Wound Repair Regen 29: 602-612, 2021.
34. Mani SA, Guo W, Liao MJ, Eaton EN, Ayyanan A, Zhou AY, Brooks M, Reinhard F, Zhang CC, Shipitsin M, *et al*: The epithelial-mesenchymal transition generates cells with properties of stem cells. Cell 133: 704-715, 2008.
35. Yang Y, Zhao B, Lv L, Yang Y, Li S and Wu H: FBXL10 promotes EMT and metastasis of breast cancer cells via regulating the acetylation and transcriptional activity of SNAI1. Cell Death Discov 7: 328, 2021.
36. López-Moncada F, Torres MJ, Lavanderos B, Cerda O, Castellón EA and Contreras HR: SPARC induces E-cadherin repression and enhances cell migration through Integrin αvβ3 and the transcription factor ZEB1 in prostate cancer cells. Int J Mol Sci 23: 5874, 2022.
37. Xiong Y, Lai X, Xiang W, Zhou J, Han J, Li H, Deng H, Liu L, Peng J and Chen L: Galangin (GLN) suppresses proliferation, migration, and invasion of human glioblastoma cells by targeting Skp2-induced epithelial-mesenchymal transition (EMT). Onco Targets Ther 13: 9235-9244, 2020.
38. Li JL, Wang ZQ and Sun XL: MYL6B drives the capabilities of proliferation, invasion, and migration in rectal adenocarcinoma through the EMT process. Open Life Sci 15: 522-531, 2020.
39. Wu C, Xia D, Wang D, Wang S, Sun Z, Xu B and Zhang D: TCOF1 coordinates oncogenic activation and rRNA production and promotes tumorigenesis in HCC. Cancer Sci 113: 553-564, 2022.
40. Liao WT, Wang X, Xu LH, Kong QL, Yu CP, Li MZ, Shi L, Zeng MS and Song LB: Centromere protein H is a novel prognostic marker for human nonsmall cell lung cancer progression and overall patient survival. Cancer 115: 1507-1517, 2009.